Acta Oceanol. Sin., 2017, Vol. 36, No. 8, P. 42–51
DOI: 10.1007/s13131-017-1025-z
http://www.hyxb.org.cn
E-mail: hyxbe@263.net

Spatio-temporal variations of Arctic amplification and their linkage with the Arctic oscillation

WANG Yanshuo[1, 2, 3], HUANG Fei[1, 2, 3*], FAN Tingting[1, 2]

[1] Physical Oceanography Laboratory/CIMST, Ocean University of China, Qingdao 266100, China

[2] Qingdao National Laboratory for Marine Science and Technology, Qingdao 266200, China

[3] Ningbo Collabrative Innovation Center of Nonlinear Harzard System of Ocean and Atmosphere, Ningbo University, Ningbo 315211, China

Received 29 March 2016; accepted 31 August 2016

Abstract

The Arctic near-surface air temperatures are increasing more than twice as fast as the global average–a feature known as Arctic amplification (AA). A modified AA index is constructed in this paper to emphasize the contrast of warming rate between polar and mid-latitude regions, as well as the spatial and temporal characteristics of AA and their influence on atmospheric circulation over the Northern Hemisphere. Results show that AA has a pronounced annual cycle. The positive or negative phase activities are the strongest in autumn and winter, the weakest in summer. After experiencing a remarkable decadal shift from negative to positive phase in the early global warming hiatus period, the AA has entered into a state of being enlarged continuously, and the decadal regime shift of AA in about 2002 is affected mainly by decadal shift in autumn. In terms of spatial distribution, AA has maximum warming near the surface in almost all seasons except in summer. Poleward of 20°N, AA in autumn has a significant influence on the atmospheric circulation in the following winter. The reason may be that the autumn AA increases the amplitude of planetary waves, slows the wave speeds and weakens upper-level zonal winds through the thermal wind relation, thus influencing surface air temperature in the following winter. The AA correlates to negative phase of the Arctic oscillation (AO) and leads AO by 0–3 months within the period 1979–2002. However, weaker relationship between them is indistinctive after the decadal shift of AA.

Key words: Arctic amplification, Arctic oscillation, decadal shift, mid-latitude

Citation: Wang Yanshuo, Huang Fei, Fan Tingting. 2017. Spatio-temporal variations of Arctic amplification and their linkage with the Arctic oscillation. Acta Oceanologica Sinica, 36(8): 42–51, doi: 10.1007/s13131-017-1025-z

1 Introduction

As the Arctic sea ice retreats under warming conditions in summer, some of the near-surface atmospheric energy and the solar radiation that would have been reflected back to space by ice are absorbed in the upper ocean. During autumn, when the air temperatures become lower than sea surface temperatures (SST), the excess heat in the ocean would be transferred to the atmosphere and warm the lower Arctic troposphere. The heat slows down the formation of sea ice or thins out sea ice, further reducing the surface albedo of the following spring and summer and warming the air, providing a classic positive feedback named albedo-temperature feedback (Serreze and Barry, 2011; Cohen et al., 2014; Walsh, 2014). The albedo-temperature feedback plays a central role in recent Arctic amplification (AA)—a phenomenon that the Arctic near-surface air temperatures are increasing 2–3 times faster than the global average in recent decades (Screen and Simmonds, 2010; Overland et al., 2015). The AA, which was first recognized by the Swedish scientist Svante Arrhenius in 1896, has been most pronounced during autumn and early winter (Arrhenius, 1896; Serreze and Barry, 2011; Screen et al., 2012).

In recent years, the Arctic is at the forefront in climate change research. An increasing number of scholars are focusing on the impact of AA on mid-latitude weather and climate. Researchers have proposed two main mechanisms to describe the connection between the changes in Arctic and mid-latitude from the perspective of atmospheric circulation. One is that the AA increases the amplitude of planetary waves, slows the wave speeds and weakens the upper-level zonal winds through the thermal wind relation, thus making the blocking situation occurs more frequently and increasing the probability of extreme weather events (Overland and Wang, 2010; Francis and Vavrus, 2012; Walsh, 2014; Cvijanovic and Caldeira, 2015; Overland et al., 2015). However, Hopsch et al. (2012) showed that the relationship between the autumn sea ice and winter atmospheric circulation is not statistically significant. Barnes (2013) suggested that the decrease in planetary-scale wave phase speeds and the increase in frequency of blocking occurrence in observations are not statistically significant over the past few decades. And another is the Arctic-midlatitude connection via Eurasian snow cover (Hopsch et al., 2012; Cohen et al., 2012; Walsh, 2014). All of these above complicate the AA effect on mid-latitude weather situation. Thus further research and better understanding are required indeed.

Arctic oscillation (AO) is the leading teleconnection pattern in sea level pressure (SLP) anomalies poleward of 20° latitude for

Foundation item: The Global Change Research Program of China under contract No. 2015CB953904; the National Natural Science Foundation of China under contract Nos 41575067 and 41376008.
*Corresponding author, E-mail: huangf@ouc.edu.cn

the Northern Hemisphere. Over the last decade, severe weathers occurred more frequently and lasted longer over mid-latitude than the 1990s, corresponding to a more dominant negative phase of the AO (Cohen et al., 2014; Kim et al., 2014; Overland et al., 2015). AA may contribute to the shift toward a negative AO (Alexander et al., 2004; Jaiser et al., 2012). The primary goal of this study is to quantify the AA and reveal the relationship between the AA and AO. So we propose a new AA index (AAI) to measure the intensity of the AA by taking the Arctic-midlatitude temperature contrasts into account. Section 2 outlines the utilized reanalysis datasets. Section 3 defines the AAI and uses it to delineate the spatio-temporal variations of AA. Section 4 further explores the associations with the atmospheric circulation. Finally, conclusions and discussion are provided in Section 5.

2 Data and methods

The primary dataset used in this study is the ERA-Interim (Dee et al., 2011), which is offered by the European Centre for Medium-Range Weather Forecasts (ECMWF). Monthly mean 2-m air temperatures (T2M), SLP, 500 hPa geopotential height, 200 hPa zonal wind, and air temperature on eight pressure levels between 1 000 and 300 hPa with a horizontal resolution of 2.5°×2.5° for the period March 1979–February 2014 are analyzed.

Time series of monthly AO index (AOI) over the period from 1950 to current used in this study is obtained from the National Oceanic and Atmospheric Administration (NOAA) Climate Prediction Center (CPC) website (http://www.cpc.ncep.noaa.gov/products/precip/CWlink/daily_ao_index/monthly.ao.index.b50.current.ascii). This index is constructed by projecting the monthly mean SLP anomalies poleward of 20°N onto the leading empirical orthogonal function (EOF) of SLP anomalies based on the NCEP/NCAR reanalysis (Thompson and Wallace, 1998). We use the AOI for the time period corresponding to the ERA-Interim reanalysis data set, viz. March 1979–February 2014. In this paper, March, April and May (MAM) are for spring, with June, July and August (JJA) for summer. September, October and November (SON) refer to autumn, and December, January and February (DJF) refer to winter. Furthermore, regarded the December in 1979 and January and February in 1980 as the winter of 1979, the rest can be done in the same manner.

3 Arctic amplification index and its spatio-temporal variations

3.1 *Arctic amplification index and its multi-timescales variations*

3.1.1 *Definition of AAI*

The northern mid-latitude land was once the world's fastest warming region (Ji et al., 2014). However, for recent two decades, Arctic warming rate turned out to be faster than the rest of the globe (Overland et al., 2015). We can also inferred from these conclusions by calculating the Arctic (60°–90°N) and northern mid-latitude (30°–60°N) area-averaged monthly mean 2 m air temperature anomaly (not shown), respectively. The correlation coefficient between these two is 0.27, which is significant at the 99% level.

It can be seen that long-term changes of the two time series are consistent by means of least square method to make linear regression for data fitting. Both of their positive climate trend coefficients are statistically significant (p<0.01), where the Arctic warming rate reaches 0.59°C/(10 a), and mid-latitude warming rate reaches 0.23°C/(10 a), and the ratio between them is about 2.6. This suggests that the near-surface air temperature averaged over the Arctic and the northern mid-latitude both have a generally significant upward trend, and the Arctic region warmed more than twice as large as the northern mid-latitude. In fact, previous studies defined the AA as the ratio of some change in Arctic temperature to a corresponding change in a mid-latitude (Screen, 2014) or global mean temperature (Juday et al., 2005; Masson-Delmotte et al., 2006; Serreze and Barry, 2011; Cohen et al., 2014). However, they can only describe AA on the decadal or even a longer time scale and sometimes extreme value occurs when the denominator is close to zero.

Based on the above analysis and taking into account the relevant definition of the AA, in order to better characterize the AA on a short time scale such as monthly and avoid extreme values, this paper constructs a new AAI, which is defined as the difference of area-averaged 2 m air temperature between the Arctic and northern mid-latitude, shown as follows:

$$ARC_t = T2M_t^{\mathrm{ar}} - T2M_m^{\mathrm{ar}}, \tag{1}$$

$$MID_t = T2M_t^{\mathrm{mi}} - T2M_m^{\mathrm{mi}}, \tag{2}$$

$$AAI_t = ARC_t - MID_t, \tag{3}$$

where $T2M$ is 2 m air temperature, ar indicates the area-averaged meteorological element over Arctic, mi indicates the area-averaged meteorological element over the northern mid-latitude, and subscript m is the climatological monthly mean. ARC_t and MID_t indicate the area-averaged 2 m air temperature anomaly over Arctic (60°–90°N) and the northern mid-latitude (30°–60°N), respectively. AAI_t represents the AAI at the t month.

Figure 1 shows the time series of AAI for the period March 1979–February 2014, where the positive index indicates strong AA. The index is a direct reflection of Arctic warming rate relative to that of the mid-latitude. To a certain extent, it can also reflect the relative rate of Arctic warming to the northern hemisphere as well as the global. In the following, a power spectrum analysis is performed to reveal the significant periods associated with this index. Before calculating this power spectrum, the linear trend has been removed.

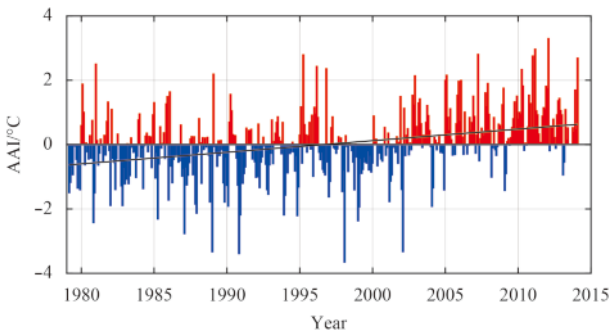

Fig. 1. Time series of monthly mean Arctic amplification index (AAI) and the linear trend of AAI (solid black line) from March 1979 to February 2014.

Figure 2 shows that there are two spectral peaks exceed the red noise spectrum at 0.05 significance level, namely the presence of two significant periods of 11.7 a and 1 a. The variation period of less than 8 a is treated as interannual variability, while

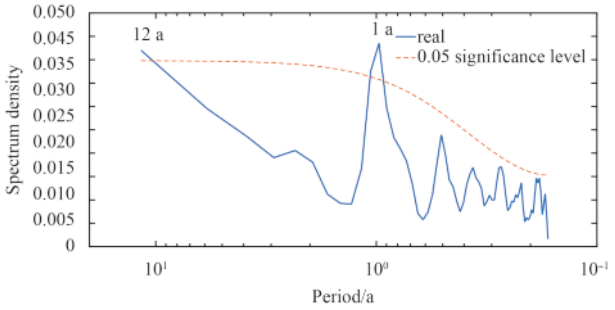

Fig. 2. Power spectrum (solid blue line) for the monthly mean AAI from March 1979 to February 2014. The red noise spectrum (red dashed line) at 0.05 significance level is also shown.

greater than or equal to 8 a is deemed as decadal variability. In that way, in addition to significant annual cycle, AAI has a 12 a quasi-decadal oscillation cycle. Nevertheless, the interannual variability of AAI is not statistically significant.

3.1.2 *Seasonal cycle of AAI*

According to Eqs (1)–(3), although both the Arctic and mid-latitude temperature curves removed their corresponding climatological seasonal cycle, the difference between these two curves still exists significant seasonal variability (Fig. 3). This might be caused by desynchronization between seasonal variability of the Arctic temperature series variance and that of mid-latitude. Figures 3c and d show the standard deviation of the area-averaged Arctic and mid-latitude T2M series from January to December, respectively. Note that the standard deviation of each calendar month in high-latitudes has a different seasonal cycle compared with that of mid-latitude. The Arctic region reaches a minimum standard deviation in July while the mid-latitude reaches in May. Figure 3b shows the difference between Fig. 3c and Fig. 3d, the amplitude variation of interannual and decadal variability in the Arctic region are larger than that in the mid-latitude for each calendar month. The seasonality of standard deviation is generally identifiable with a minimum in summer and a maximum in winter.

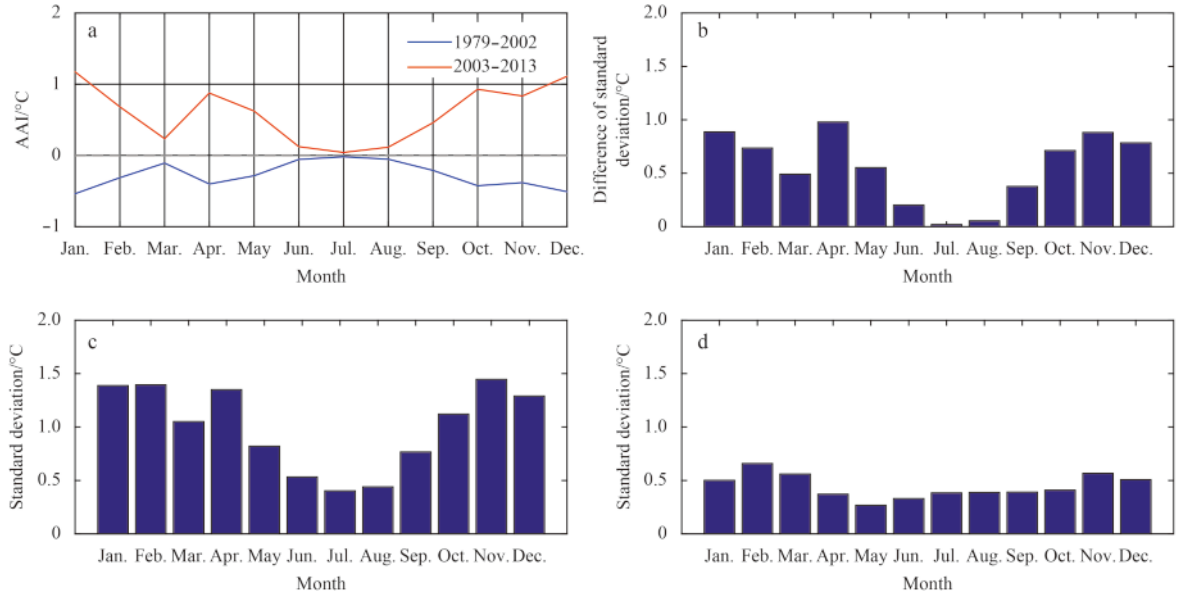

Fig. 3. Climatological seasonal cycle of AAI during 1979–2002 (solid blue line) and 2003–2013 (solid red line) (a); standard deviation of averaged T2M of Arctic region (60°–90°N) (c), mid-latitude region (30°–60°N) (d), and difference between the two regions (b).

3.1.3 *AAI variability in different seasons*

Long-term trend is an important feature which reflects the climate change. Figure 1 shows that the monthly mean AAI has a generally upward trend of 0.36°C/(10 a), and its climate trend coefficient is 0.35 which reaches 0.01 significance level. So the climate trend coefficient is significant, indicating that the AA distinctly enhanced in recent decades. Nevertheless, trends among four seasonal mean index are still showed diversity to some extent (Fig. 4). Although all seasonal mean AAI values are on the rise during past 35 a, upward trends are the strongest in autumn and the weakest in summer, and the former is nearly 11 times faster than the latter. In addition to summer, the rest three seasons all have significant upward trends.

As seen from Fig. 4, the AA exists significant seasonal variability. To be more specific, AA phenomenon performs the weakest in summer, which is basically in a neutral state with no apparent phase shift. The rest of seasons has a significant shift from negative phase to positive phase in the mid-1990s when the global warming hiatus begins. The autumn and winter AAI are located in a strong negative phase before 2000 and positive phase after 2000, respectively. The correlation coefficient between the autumn AAI and winter AAI is 0.52, far beyond 0.01 significance level. The standard deviation of AAI in winter is larger compared to that in autumn. That is, as for AAI, the seasonal variability of its phase intensity is consistent, the positive or negative phase activities are the strongest in autumn and winter, the weakest in summer. And spring is a transition season.

3.1.4 *Decadal variability of AAI*

Figure 5a shows the accumulative anomaly curve for AAI series. Overall, there is a gradually downward trend before 2002 and faster upward trend after 2002. AA starts shifting from weak to strong around 2002; the upward trend of AAI means that positive anomaly is dominant after 2002, and rising speed is almost twice the rate faster than the decline speed. One of the most significant mutations occurred in 2002 (that is the corresponding

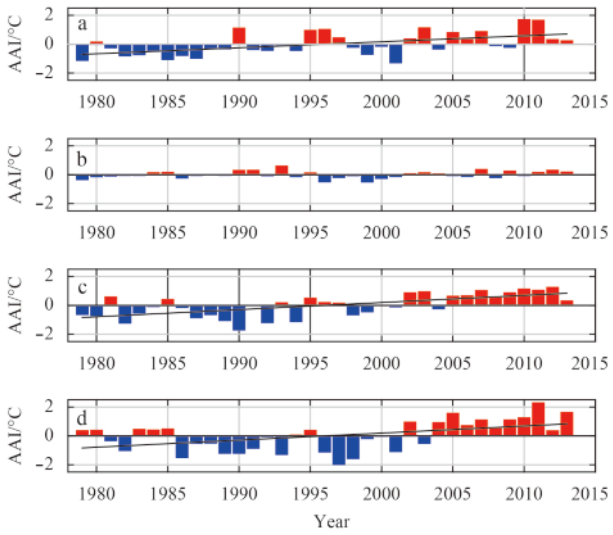

Fig. 4. Time series of seasonal mean AAI in MAM (a), JJA (b), SON (c), and DJF (d).

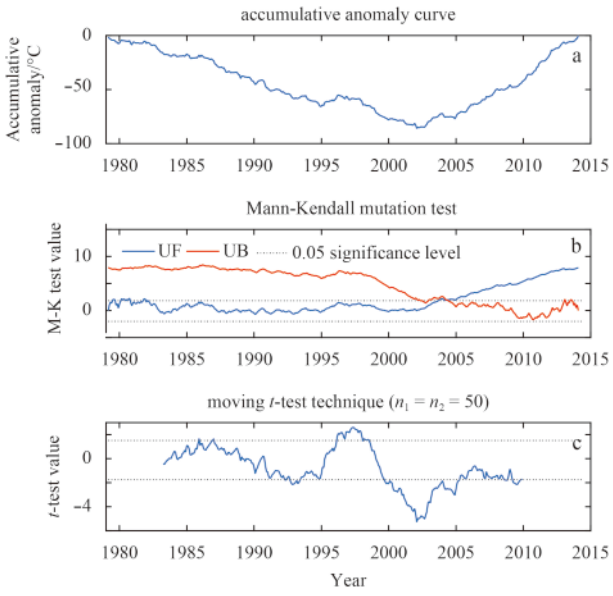

Fig. 5. The accumulative anomaly curve (a), Mann-Kendall test (b) and moving *t*-test for AAI (c). UF and UB denote sequence and inverted sequence of statistical test variables, respectively. The black dotted lines are at the 0.05 significance level.

time to the valley in Fig. 5a), which can also be seen in the moving *t*-test, but the mutation time Mann-Kendall test showed a slight delay in 2004. So we can conclude that decadal regime shift of AA occurred during 2002–2004, and this shift is consistent with the feature of autumn decadal variability (not shown), in other words, the decadal regime shift of AA is affected mainly by decadal shift in autumn. Global mean temperature has levelled off since 1998, that is, into a period of global warming hiatus (IPCC, 2013). In this context, after experiencing a remarkable decadal shift from negative phase to positive phase in the early global warming hiatus period, the AA has entered into a state of being enlarged continuously. It is noteworthy that the Arctic sea ice loss accelerated in 1997 (Huang et al., 2014), leading the decadal regime shift of AA by 5 a. To a certain extent, this feature is qualitatively consistent with the perspective that diminishing sea ice plays an important role in recent AA proposed by Screen and Simmonds (2010). In addition, AAI also had a significant mutation in 1996/1997. There is a relatively clear upward trend during 1995–1996, in this period AAI express mainly positive anomaly, showed negative anomaly again in subsequent years (Figs 5a and c).

According to decadal regime shift of AA, the AA can be divided into two periods: 1979–2002 and 2003–2013. It can be seen from Fig. 3a that AA is at the negative phase during the first period and positive phase during the second period. The decadal variations in the seasonality of AAI appear inconsistent features in different seasons (Fig. 6). The interdecadal shift at about 2002 of the AA phenomenon appears much more apparent in autumn and winter seasons, with more negative values exhibited during 1987–1998 and much more positive values after the year of 2000.

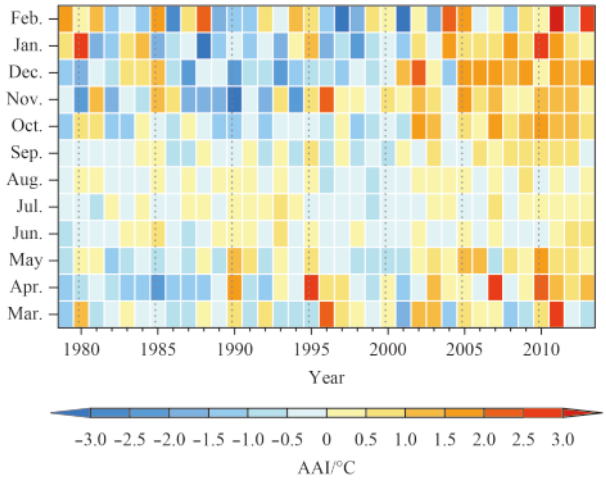

Fig. 6. Time series of monthly mean AAI from March 1979 to February 2014.

3.2 *Spatial distribution features of AA*

3.2.1 *Horizontal pattern of AA*

To show the horizontal pattern of AA, the monthly T2M anomalies fields are regressed onto the AA index from 1979 to 2013 (Fig. 7a). When the AAI has an overall upward trend, the Arctic and mid-latitude land temperatures show obvious abnormalities. Most of the Arctic region shows obvious positive anomalies, especially in the Barents and Kara Seas. Furthermore, the Eurasian continent and North American continent, which are located in the middle latitudes, have obvious negative anomalies centers.

Regression maps of the monthly mean T2M anomalies fields onto the AAI for period of 1979–2002 and 2003–2013 are shown in Figs 7b and c, respectively. It seems a little bit different in the distribution of positive and negative anomalies between the two periods. During 1979–2002, the Mongolia to the south of Lake Baikal and the Great Lakes in North America both have clear negative anomalies centers. The positive anomalies centers are located in the Barents-Kara Seas region and Chukchi-Beaufort Seas region, that is, upstream of the negative anomalies centers. By comparing results before and after 2002, we can find that the anomalies centers of the Western Hemisphere weaken while those of the Eastern Hemisphere enhance. The negative anomalies center which is located at Mongolia during the first period extends westward to the Black Sea, southeastward to the coastal margin of southeast China during the second period. The posit-

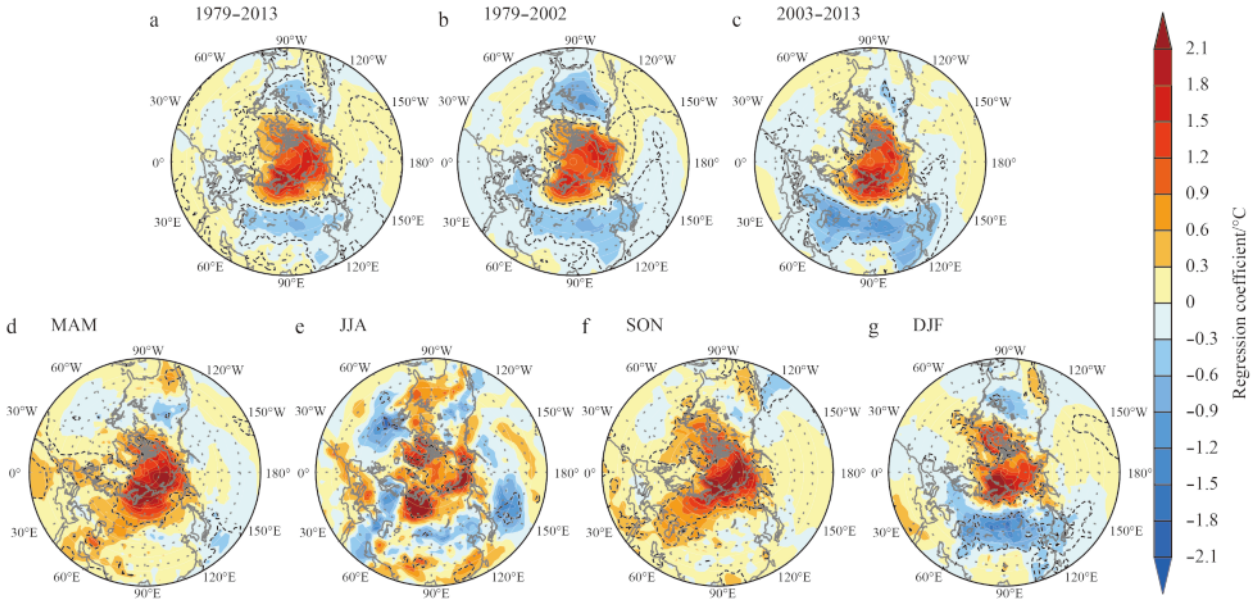

Fig. 7. Surface air temperature anomalies regressed by the monthly mean AAI during 1979–2013 (a), 1979–2002 (b) and 2003–2013 (c); and by seasonal mean AAI in MAM (d), JJA (e), SON (f) and DJF (g). The areas where the confidence level exceeds 95% are surrounded by black dotted lines.

ive anomalies center in the Barents-Kara Seas region moves northward to near 80°N and expands larger than its original range.

Regression maps of seasonal mean T2M anomalies fields on the AAI for four seasons exhibit similar features. The positive anomalies mainly span the whole Arctic region and the negative anomalies mainly in mid-latitude, but the location of their anomalies centers still show regional differences (Figs 7d–g). In spring, autumn and winter, positive anomalies centers have emerged near the Eurasian continent in the Arctic region. In summer, by contrast, the positive anomalies centers are decentralized, including two positive anomalies centers appeared in the south of Novaya Zemlya and the east of Bering Strait. Comparing with the other seasons, these two centers that located in the Eurasian continent are further south. Additionally, the Greenland region also has a positive anomalies center which is not found in other seasons. The negative anomalies are not obvious in spring and autumn. In summer, the northwest Pacific and northwest Atlantic exhibit significant negative anomalies. There is a wide range of negative anomalies appeared in the interior of Eurasian continent in winter.

3.2.2 *Vertical structure of AA*

To further illustrate the changes in tropospheric air temperatures that occur in response to changes in the amplitude and polarity of the near surface AA, the air temperatures fields on pressure surfaces from 1 000 to 300 hPa are regressed onto the AAI (Fig. 8). Figure 8a shows that the maximum positive anomalies located around 80°N in the Arctic has significant weakening with increasing altitude, which illustrates that the AA shows a trend to spread from near surface to the upper atmosphere overall.

The spread of warming at different longitudes behaves differently (Fig. 8b), which are highlighted in the Arctic Ocean around the Bering Strait. Considering that the Bering Strait is located between the Bering Sea and Chukchi Sea and it is the only way to connect the Pacific and the Arctic Ocean, this regional differences may be related to the air-sea poleward transport of heat from the North Pacific. Minor positive anomalies centers are located in the vicinity of the Baffin Bay and to the north of the Novaya Zemlya.

The regression fields of all seasons (Figs 8c–j) show that positive anomalies in the Arctic troposphere are the strongest in summer and the weakest in winter. It is noteworthy that the maximum positive anomalies are at surface of the Arctic region and those positive anomalies lessen with height in all seasons except summer. In summer, positive anomalies center appeared near 900 hPa, which may be due to the modest near-surface warming, as the heat is used to melt remaining sea ice and be absorbed in the upper ocean (Screen and Simmonds, 2010). In addition, it is also somewhat different from other seasons that the positive anomalies centers of different altitudes shift poleward with height in summer. As previously explained, the summer AAI has no significant upward trend, which is different from the rest seasons. The rate of rise in autumn is almost 11 times faster than that in summer, so the characteristics of spatial regression fields that the positive anomalies are the strongest in summer and the weakest in winter can be attributed to the higher sensitivity of the summer air temperature to the AAI. Furthermore, the southward shift of maximum positive anomalies in winter is consistent with the southward migration of the sea ice edge from autumn to winter (Walsh, 2014).

4 Associated atmospheric circulation with AA

4.1 *Autumn-winter atmospheric circulation associated with autumn AA variability*

The AA occurs in all seasons, but is most pronounced in autumn and early winter (Serreze et al., 2009; Screen et al., 2013; Perlwitz et al., 2015), especially in the recent decade (Figs 3a and 6). The correlation coefficient between the AAI in autumn and in winter for the period 1979–2013 is far beyond the 0.01 significance level (r=0.52). Therefore, we will mainly focus on the autumn AA influence to examine the autumn and the following winter atmospheric response.

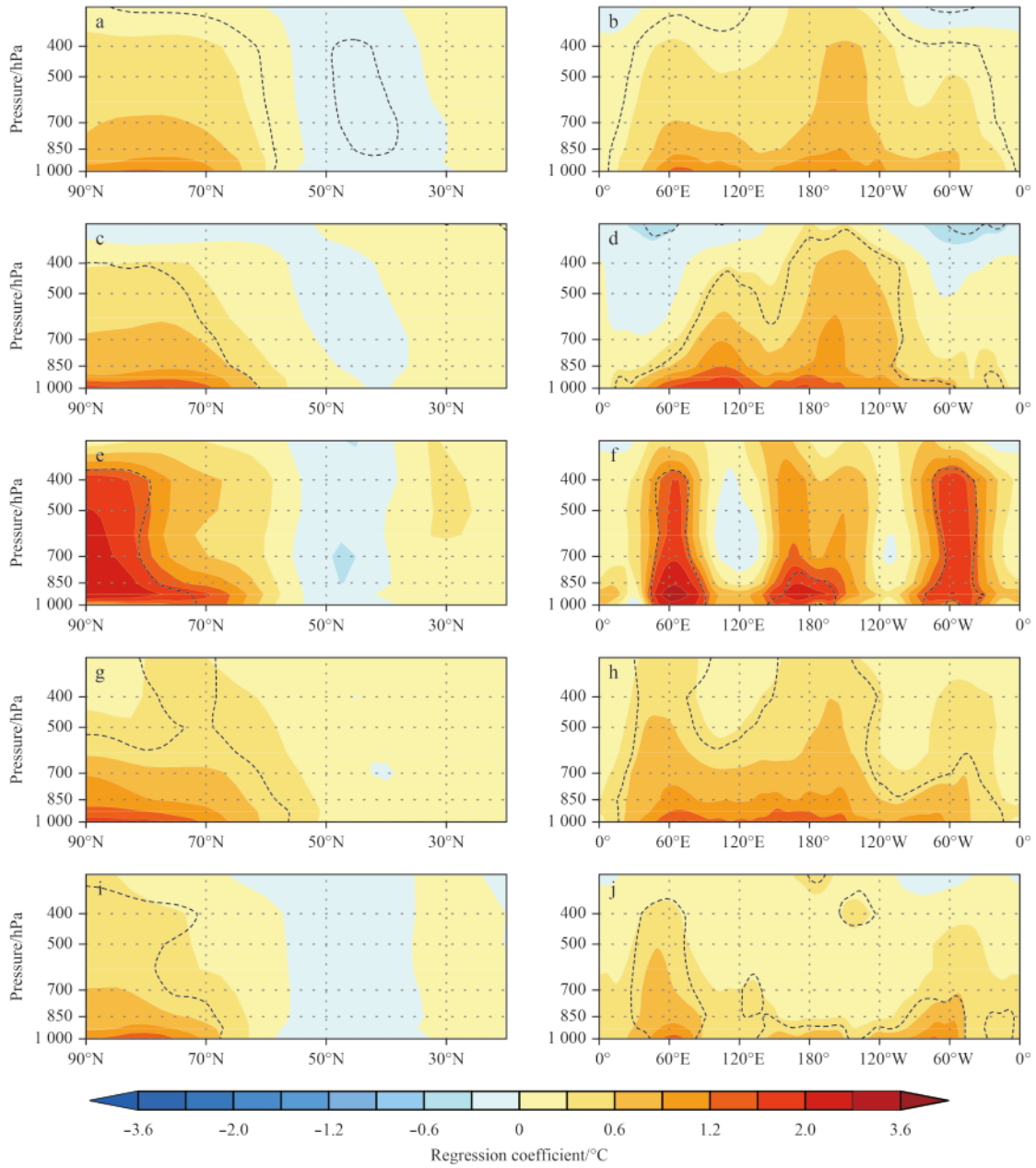

Fig. 8. Latitude-height cross-section of regression between air temperature anomalies and monthly mean AAI (a) or seasonal mean AAI in MAM (c), JJA (e), SON (g) and DJF (i); and longitude-height cross-section of regression coefficient averaged from 60° to 90°N between air temperature anomalies and monthly mean AAI (b) or seasonal mean AAI in MAM (d), JJA (f), SON (h) and DJF (j). The areas where the confidence level exceeds 95% are surrounded by black dotted lines.

Regression maps of the seasonal mean fields of T2M and SLP onto the autumn AAI for autumn and winter are shown in Figs 9a, b, c, and d. In addition to the North Atlantic sector, the T2M anomalies over the Arctic are positive in autumn, and two centers of them are located in the Kara Sea and Chukchi Sea. The positive SLP anomalies centers are located in north of the Beaufort Sea, the Ural Mountains and south of the Greenland, but they are all insignificant. In the following winter, T2M fields in the Barents Sea and near Baffin Island have significant positive anomalies centers, while west of Lake Baikal, high latitudes of eastern Eurasia and the interior of North America appear negative anomalies centers. From Greenland eastward to Novaya Zemlya, positive SLP anomalies appear over the Arctic region and the negative SLP anomalies locate in the mid-latitude from Atlantic to east coast of the North American. The North Atlantic and Western Europe show a north–south-oriented dipole distribution, resembling the negative phase of the North Atlantic Oscillation (NAO), which manifest both weakened Icelandic low and Azores High (Serreze et al., 1997). Meanwhile the Greenland High and cold high to the northwest of Lake Baikal are reinforced.

In the mid-troposphere, a remarkable feature is the positive geopotential height anomalies (GHA) spanning the whole Arctic region in autumn (Fig. 9e), and the anomalies center is located in the Pacific sector of the Arctic. The GHA of Davis Strait and the Ural Mountains have significant positive anomalies centers, and

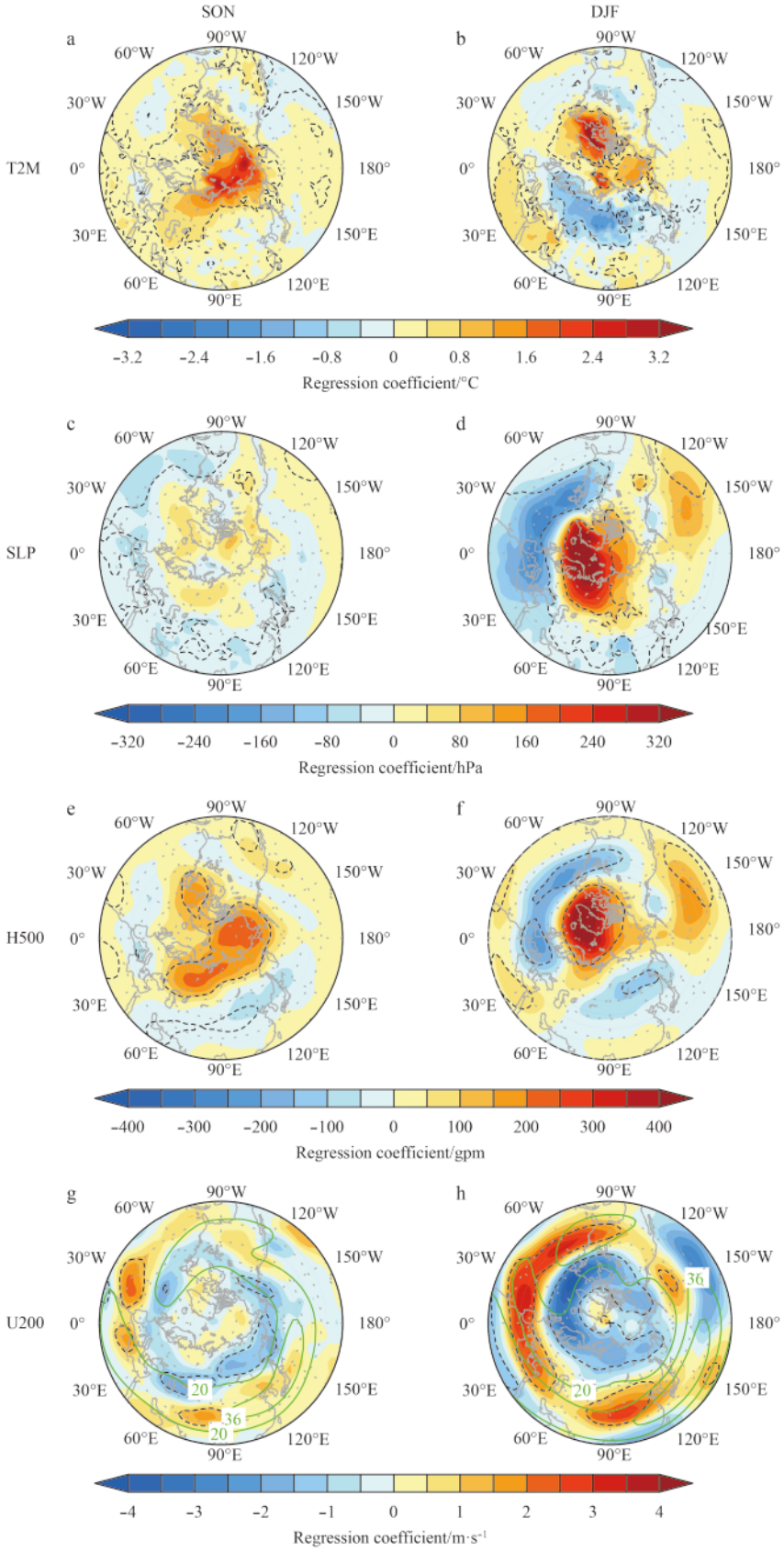

Fig. 9. The regression between autumn AAI and the corresponding autumn (SON), and following winter (DJF) 2 m air temperature (a and b), sea level pressure (c and d), 500-hPa geopotential height (e and f) and 200-hPa zonal wind (g and h). The areas where the confidence level exceeds 90% are surrounded by black dotted lines. In Figs 9g and h, climatological 200 hPa jet stream are surrounded by solid green lines.

the former is more powerful than the latter, extending southward to around 50°N. The GHA in the Mediterranean region and south of the Lake Baikal appear significant negative anomalies centers, making the circulation pattern resemble negative phase of AO overall. In the following winter, the GHA over the Greenland and around Iceland exhibits strong positive centers which are significant and extended eastward to the central Barents Sea (Fig. 9f). Significant negative anomalies center appears west of the Azores, which is consistent with the regression fields of SLP exhibiting clear NAO-like anomalies (Fig. 9d). At the same time the Gulf of Alaska has a weak negative anomalies center, north of the Hawaiian Islands has a significant positive anomalies center. The four anomalies centers mentioned above correspond to the four active centers of the Pacific/north American pattern (PNA) defined by Wallace and Gutzle (1981). The locations of overall centrals slightly skew northeastward, showing the positive phase of the PNA-like wave train structure. Significant negative anomalies centers appear over the Western Europe and the Siberia in east of the Lake Baikal.

Compared to the climatological 500 hPa geopotential height fields in autumn and winter, we can find that the weak ridge located at the Ural Mountains in autumn extends northward, and the troughs over East Asian and North America weaken and move westward. In the following winter, both the East Asia trough moving westward and the North America trough extending southwestward become deeper, indicating that the autumn AA plays a stronger influence on the 500 hPa geopotential height in the regions including the middle latitudes of East Asian and North America in winter than that in autumn.

In the upper troposphere, compared with the climatological 200 hPa jet stream surrounded by solid green lines shown in Figs 9g and h, it can be inferred that the westerly jet accelerates over the Tibet Plateau, which is south of the northern Eurasian continent where the zonal wind has a significant negative anomalies. In the following winter, the westerly jet located on the eastern coast of the North American continent accelerates and moves southeastward. The westerly jet spans from the western Europe to the central Pacific in the longitudinal direction, accelerates over the North Africa, the Middle East and China, making the position of the jet stream move slightly northward. Moreover, the significant easterly wind anomalies are observed north of the jet stream.

The circulation situation during winter is consistent with the pattern of the high-latitude blocking (HLB) events (Davini, 2013). Lied north of the climatological jet stream position, HLBs tend to divert the jet stream southward rather than completely blocking the westerly winds (Overland et al., 2015), which induce the zonal winds accelerates in the south and slows down in the north, increase the amplitude of planetary waves, and thus favor increased frequence of cold-air outbreaks and associated extreme weathers over mid-latitude in winter.

4.2 *Lead-lag correlation between AA and AO*

The previous section illustrates that the autumn AA has a significant influence on the atmospheric circulation of Northern Hemisphere in the following winter. The leading principal component of the wintertime atmospheric circulation anomaly is the AO, which well reflects the atmospheric response to the lower interface. It could be inferred that the autumn AA might affect the winter AO from the correlation coefficient between the autumn AAI and the winter AOI for the period 1979–2013, which is far beyond the 0.01 significance level.

To further illustrate the relationship between AA and AO, lead-lag correlation analysis is performed (Fig. 10). Figure 10a shows that the correlation between the AA and AO is significantly negative when AA leads AO by 0–3 months. The maximum significant correlation (above the 0.05 significance level) is about –0.20 when AA leads AO by 2 months. This relationship indicates that the AA can affect the atmospheric circulation from the same period to the following one season, thereby influencing the AO. Figures 10b and c show lead-lag relationships between the AAI and AOI during the periods 1979–2002 and 2003–2013, respectively. As shown in Figs 10b and c, the lead-lag correlations during 1979–2002 are similar to that shown in Fig. 10a, but not for period 2003–2013. During 2003–2013, the negative correlation reaches a maximum when the AA leads AO by 2 months, nevertheless, it is not remarkable. These results imply that the relationship between AA and AO reduce after the decadal regime shift of AA, suggesting that the decoupling between AO and sea ice in recent decades (Zhang et al., 2008) is likely to cause the shift according to the view that the diminishing sea ice plays an important role in recent AA (Screen and Simmonds, 2010).

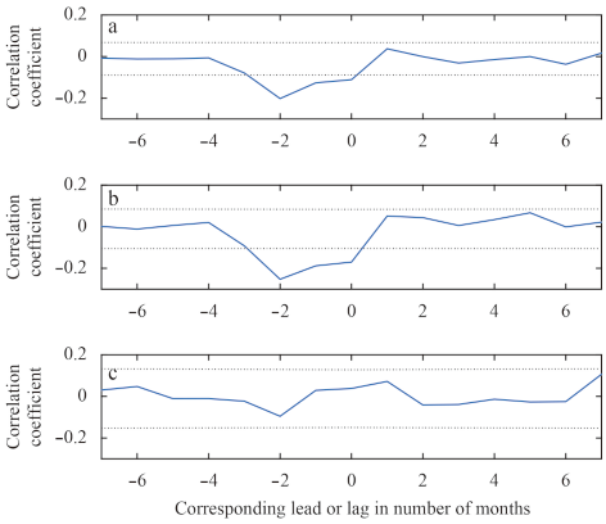

Fig. 10. Lead-lag correlations between the AAI and AOI during 1979–2013 (a), 1979–2002 (b) and 2003–2013 (c). The number along the *x*-axis indicates the corresponding lead or lag in number of months, positive numbers correspond to the case where AA lags AO whereas negative numbers is when AA leads AO. The black dotted lines are at the 0.05 significance level.

5 Conclusions and discussion

This paper constructs an index, AAI, which is defined as the difference between Arctic region and northern mid-latitude area-averaged monthly mean 2 m air temperature anomalies. The index can well reflect the rate of Arctic warming relative to that of the mid-latitude. In addition to significant annual cycle, AAI has a 12 a quasi-decadal oscillation cycle. Nevertheless, the interannual variability of AAI is not statistically significant. The upward trend of monthly mean AAI is significant, indicating that the AA distinctly enhanced in recent decades. However, trends among four seasonal mean indexes are still showed diversity. The upward trends are the strongest in autumn and the weakest in summer, and the warming rate in autumn is nearly 11 times faster than that in summer. As for the seasonal variability of AAI, the positive or negative phase activities are the strongest in autumn and winter, the weakest in summer. And spring is a transition season. After experiencing a remarkable decadal shift from negative phase to positive phase in the early global warming hiatus

period, the AA has entered into a state of being enlarged continuously, and the decadal regime shift of AA is affected mainly by decadal shift in autumn. According to decadal regime shift of AA, the AA can be divided into two periods: 1979–2002 and 2003–2013. AA is on the negative phase during the first period and positive for the second period. The AA phenomenon shows no significant seasonal transfer trend among different seasons during the two periods. In the spatial pattern of AA, the positive anomalies mainly span the whole Arctic region and the negative anomalies are mainly in mid-latitude during 1979–2013, but there are regional differences between two periods and among four seasons. In terms of vertical structure, the AA shows a trend to spread from near surface to the upper atmosphere overall, and the spread at different longitudes behaves differently.

The autumn AA has a significant influence on the atmospheric circulation of Northern Hemisphere in the following winter. In the mid-troposphere, the East Asia trough moves west, meanwhile, the North America trough extends southwestward and becomes deeper. In the upper troposphere, the westerly jet located on the east coast of the North American continent accelerates and moves southeastward. The westerly jet spans from Western Europe to the central Pacific in the longitudinal direction, accelerates over North Africa, the Middle East and China, making the position of the jet stream move slightly northward. Moreover, the significant easterly wind anomalies are observed north of the jet stream. The lead-lag correlations demonstrate that the AA leads the AO by 0–3 months within the entire 1979–2013, and the similar phenomenon could be seen in period 1979–2002, but not in period 2003–2013.

Recent cooling is localized over the central Eurasia and eastern United States, indicating that a variety of mechanisms may be operating at different longitudes and thus may be obscured by analyses based on zonal averaging (Screen and Simmonds, 2014; Perlwitz et al., 2015). Depending on geographical area, certain types of extreme weather are more strongly correlated with wave amplitude changes than others. Screen and Simmonds (2014) suggested a way forward through a study of regional and seasonal mechanisms. Therefore, regional AAIs should be established to learn more detailed characteristics of regional Arctic amplification effect, based on the difference between the East Asia and North America and their associated upstream Arctic warming regions, respectively.

The low frequency variability including the Northern Hemisphere Mode (NAM; Wallace, 2000) and Pacific Decadal Oscillation (PDO; Mantua et al., 1997) in the Arctic system complicates the characteristics of AA (Serreze and Francis, 2006; Perlwitz et al., 2015). Moreover, regional Arctic warming might be primarily due to the forcing by the SST changes remotely (Ding et al., 2014). These calls for an enhanced understanding of the role of processes outside the Arctic played in AA, especially the contribution of tropical mechanisms.

References

Alexander M A, Bhatt U S, Walsh J E, et al. 2004. The atmospheric response to realistic Arctic sea ice anomalies in an AGCM during winter. J Climate, 17(5): 890–905

Arrhenius S. 1896. On the influence of carbonic acid in the air upon the temperature of the ground. Philos Mag J Sci, 41(251): 237–276

Barnes E A. 2013. Revisiting the evidence linking Arctic amplification to extreme weather in midlatitudes. Geophys Res Lett, 40(17): 4734–4739

Cohen J L, Furtado J C, Barlow M A, et al. 2012. Arctic warming, increasing snow cover and widespread boreal winter cooling. Environ Res Lett, 7(1): 014007

Cohen J, Screen J A, Furtado J C, et al. 2014. Recent Arctic amplification and extreme mid-latitude weather. Nat Geosci, 7(9): 627–637

Cvijanovic I, Caldeira K. 2015. Atmospheric impacts of sea ice decline in CO_2 induced global warming. Climate Dyn, 44(5–6): 1173–1186

Davini P. 2013. Atmospheric blocking and winter mid-latitude climate variability [dissertation]. Venice: Università Ca'Foscari Venice

Dee D P, Uppala S M, Simmons A J, et al. 2011. The ERA-Interim reanalysis: configuration and performance of the data assimilation system. Quart J Roy Meteor Soc, 137(656): 553–597

Ding Qinghua, Wallace J M, Battisti D S, et al. 2014. Tropical forcing of the recent rapid Arctic warming in northeastern Canada and Greenland. Nature, 509(7499): 209–212

Francis J A, Vavrus S J. 2012. Evidence linking Arctic amplification to extreme weather in mid-latitudes. Geophys Res Lett, 39(6): L06801

Hopsch S, Cohen J, Dethloff K. 2012. Analysis of a link between fall Arctic sea ice concentration and atmospheric patterns in the following winter. Tellus A, 64(1): 18624

Huang Fei, Di Hui, Hu Beibei, et al. 2014. Decadal regime shift of arctic sea ice and corresponding changes of extreme low temperature. Climate Change Research Letters (in Chinese), 3(2): 39–45

IPCC (Intergovernmental Panel on Climate Change). 2013. Summary for policymakers. In: Stocker T F, Qin D, Plattner G K, et al., eds. Climate Change 2013: the Physical Science Basis. Contribution of Working Group I to the Fifth Assessment Report of the Intergovernmental Panel on Climate Change. United Kingdom, New York, USA: Cambridge University Press

Jaiser R, Dethloff K, Handorf D, et al. 2012. Impact of sea ice cover changes on the Northern Hemisphere atmospheric winter circulation. Tellus A, 64(1): 11595

Ji Fei, Wu Zhaohua, Huang Jianping, et al. 2014. Evolution of land surface air temperature trend. Nat Climate Change, 4(6): 462–466

Juday G P, Barber V, Vaganov E, et al. 2005. Forests, land management, and agriculture. In: Arctic Climate Impact Assessment. Cambridge: Cambridge University Press, 781–862

Kim B M, Son S W, Min S K, et al. 2014. Weakening of the stratospheric polar vortex by Arctic sea-ice loss. Nat Commun, 5: 4646

Mantua N J, Hare S R, Zhang Yuan, et al. 1997. A Pacific interdecadal climate oscillation with impacts on salmon production. Bull Amer Meteor Soc, 78(6): 1069–1079

Masson-Delmotte V, Kageyama M, Braconnot P, et al. 2006. Past and future polar amplification of climate change: climate model intercomparisons and ice-core constraints. Climate Dyn, 26(5): 513–529

Overland J E, Francis J, Hall R, et al. 2015. The melting Arctic and midlatitude weather patterns: are they connected?. J Climate, 28(20): 7917–7932

Overland J E, Wang Muyin. 2010. Large-scale atmospheric circulation changes are associated with the recent loss of Arctic sea ice. Tellus A, 62(1): 1–9

Perlwitz J, Hoerling M, Dole R. 2015. Arctic tropospheric warming: causes and linkages to lower latitudes. J Climate, 28(6): 2154–2167

Screen J A. 2014. Arctic amplification decreases temperature variance in northern mid-to high-latitudes. Nat Climate Change, 4(7): 577–582

Screen J A, Deser C, Simmonds I. 2012. Local and remote controls on observed Arctic warming. Geophys Res Lett, 39(10): L10709

Screen J A, Simmonds I. 2010. The central role of diminishing sea ice in recent Arctic temperature amplification. Nature, 464(7293): 1334–1337

Screen J A, Simmonds I. 2014. Amplified mid-latitude planetary waves favour particular regional weather extremes. Nat Climate Change, 4(8): 704–709

Screen J A, Simmonds I, Deser C, et al. 2013. The atmospheric re-

sponse to three decades of observed Arctic sea ice loss. J Climate, 26(4): 1230–1248

Serreze M C, Barrett A, Stroeve J, et al. 2009. The emergence of surface-based Arctic amplification. Cryosphere, 3(1): 11–19

Serreze M C, Barry R G. 2011. Processes and impacts of Arctic amplification: a research synthesis. Glob Planet Change, 77(1–2): 85–96

Serreze M C, Carse F, Barry R G, et al. 1997. Icelandic low cyclone activity: climatological features, linkages with the NAO, and relationships with recent changes in the Northern Hemisphere circulation. J Climate, 10(3): 453–464

Serreze M C, Francis J A. 2006. The Arctic amplification debate. Climatic Change, 76(3–4): 241–264

Thompson D W J, Wallace J M. 1998. The Arctic oscillation signature in the wintertime geopotential height and temperature fields. Geophys Res Lett, 25(9): 1297–1300

Wallace J M. 2000. North Atlantic Oscillation/annular mode: two paradigms-one phenomenon. Quart J Roy Meteor Soc, 126(564): 791–805

Wallace J M, Gutzler D S. 1981. Teleconnections in the geopotential height field during the Northern Hemisphere winter. Mon Wea Rev, 109(4): 784–812

Walsh J E. 2014. Intensified warming of the Arctic: causes and impacts on middle latitudes. Glob Planet Change, 117: 52–63

Zhang Xiangdong, Sorteberg A, Zhang Jing, et al. 2008. Recent radical shifts of atmospheric circulations and rapid changes in Arctic climate system. Geophys Res Lett, 35(22): L22701